Available online at www.sciencedirect.com
SCIENCE DIRECT
ELSEVIER
Journal of the European Ceramic Society 26 (2006) 915–921
ECERS
www.elsevier.com/locate/jeurceramsoc

Sol–gel auto-igniting synthesis and structural property of cerium-doped titanium dioxide nanosized powders

Qing-Zhi Yan[a,*], Xin-Tai Su[a], Zhen-Ying Huang[b], Chang-Chun Ge[a]

[a] *Laboratory of Special Ceramics and Powder Metallurgy, University of Science and Technology Beijing, Beijing 100083, PR China*
[b] *College of Mechanical Electronic and Control Engineering, Beijing Jiaotong University, Beijing 100044, PR China*

Received 2 July 2004; received in revised form 15 November 2004; accepted 21 November 2004
Available online 20 April 2005

Abstract

Anatase-type TiO_2 (titania) doped with cerium up to 5 mol% was directly formed as nanometer-sized particles from $TiO(NO_3)_2$–$Ce(NO_3)_2$–NH_4NO_3–citric acid complex compound system by sol–gel auto-igniting synthesis process. The precursor gel was characterized by infrared spectroscopy and TG/DSC analysis. The XPS measurement showed that Ce(III) was easily oxidized to Ce(IV) at 550 °C and above. The XRD data, XPS spectra, and TEM selected-area diffraction patterns confirmed that cerium(IV) formed a solid solution in the anatase-type TiO_2 powders. Doping of CeO_2 into TiO_2 shifted the phase transformation from anatase- to rutile-type structure to a high temperature. On the other hand, CeO_2 was segregated on the surface of TiO_2 and the rutile formation was accelerated during phase transformation from anatase to rutile at elevated temperature. When the cerium content was increased in the anatase phase, onset of optical absorption shifted to longer wavelengths, and absorption in the UV-light region and in the visible-light region over 400–500 nm clearly appeared in the diffuse reflectance spectra of the as-prepared Ce-doped TiO_2.

Keywords: Sol–gel processes; TiO_2; Powder preparation; Optical properties

1. Introduction

Titanium dioxide has been the subject of numerous studies because of its many useful optical, electrical, and photocatalytic properties, which depend on the phase composition, microstructure, and chemical composition.[1–4] It is well known that titania has three crystalline forms of anatase (tetragonal), rutile (tetragonal), and brookite (orthorhombic). Among these crystalline forms, anatase phase has received considerable attention because of its photochemical properties as catalysts for photodecomposition and solar energy conversion.[5–8] Because TiO_2 absorbs only near-ultraviolet (UV) light, doping of metal ions into TiO_2 has been investigated to extend the absorption threshold to the visible-light region for better photocatalytic performance. Metal ion dopants in TiO_2 modifies strongly the anatase–rutile phase transition temperature,[9] changes the photoreactivity of TiO_2 nano-sized particles,[10–13] and enhances the catalytic properties of supported metals or oxides.[12] Various synthetic routes like the mixed-oxide process,[14,15] hydrothermal route,[7] sol–gel route[16–19] and wet impregnation[2,20] have been studied for doped TiO_2 powders. Among those, the sol–gel process leads to the greatest possible homogeneous distribution of the dopant in the host matrix and high surface area TiO_2 particles.[12,13] However, the drawback of the mentioned sol–gel route is the application of expensive raw material of tetra-isopropylorthotitanate and organic solvent, which was limited.

In this work, we focus on the synthesis of pure and doped TiO_2 powders by a sol–gel autoignition synthesis (SAS) process—a novel way and unique combination of the combustion process and the chemical gelation process. This

* Corresponding author. Tel.: +86 62332472; fax: +86 62332472.
E-mail address: yqz_2007@sina.com (Q.-Z. Yan).

0955-2219/$ – see front matter © 2005 Elsevier Ltd. All rights reserved.
doi:10.1016/j.jeurceramsoc.2004.11.017

method has been used successfully for the preparation of CeO_2,[21] $BaTiO_3$,[22] and Ni-YSZ cermet.[23] The SAS process exploits the advantages of inexpensive precursors, mixing of compositions at the level of atoms or molecules, synthesizing of ultrafine, homogeneous highly reactive powder, and simple preparation method. Starting with the solution of all components, the best process conditions and various ratios of the intimately mixed materials can be readily achieved.[24–26]

Besides, we chose cerium ion as dopant because it is an efficient electron acceptor to remove photogenerated electrons from the electron–hole recombination sites, increasing quantum yield rate.[27] Wide compositional Ce-doped TiO_2 powder with single-phase anatase form structure was directly formed as nanometer-sized particles by simple SAS process from $TiO(NO_3)_2$–$Ce(NO_3)_2$–citric acid (CA) based complex compound system. The valence of cerium in the powder and the influence of cerium contents on the crystal size, lattice parameters, phase transformation from anatase to rutile, and diffuse reflectance spectra of samples were systemically investigated.

2. Experimental procedure

The raw materials $TiCl_4$, $Ce(NO_3)_2$ and $C_6H_7O_8{\cdot}H_2O$ (citric acid, CA) used are reagent grade purity. $TiO(NO_3)_2$ as the source of titanium was prepared from $TiCl_4$ according to the following procedure: $TiCl_4$ was dissolved in cold distilled water to hydrolyze, then $TiO_2{\cdot}nH_2O$ was precipitated by the addition of excess aqueous ammonia. After filtration, the precipitate was washed with distilled water until free of Cl^- ions. The precipitate was dissolved by different amount of concentrated HNO_3. The content of Ti^{4+} in the titanyl solution was measured by complexometric titration.[28]

CA was dissolved in distilled water and mixed with titanium oxynitrate solution. The molar ratios of CA/Ti and NO_3/CA were kept constant at 2 and 3. After adjusting the pH value with ammonia to 6–7, the mixture solution was evaporated at 70–100 °C to gradually form a clear organic or brown-colored gel, i.e., precursor gel. In case of doped titania, the synthesis starts with the dissolving of respective amount of cerium nitrate in the mixture solution of CA and $TiO(NO_3)_2$. For the preparation of the powders, the precursor gel was baked at 150 °C in muffle furnace and expanded, then was auto-ignited at about 250 °C. The puffy, porous gray powders as-combusted were calcined at the temperature of 550–1000 °C for 2 h in air. By this procedure powders with cerium concentration from 0 to 100 mol% were obtained. These powders are characterized by X-ray diffraction, infrared spectroscopy, field emission scanning electron microscopy, transmission electron microscopy, X-ray photoelectron spectroscopy, UV–vis absorption spectra and various thermal analyses.

The crystallite size of anatase was estimated from the line broadening of the (2 0 0) diffraction peak, according to the Scherrer equation. The lattice parameters were measured using silicon as the internal standard. The amount of rutile phase formed in the heated samples were calculated from the equation[29]

$$X_R = \frac{1}{1 + 0.79 I_a / I_r}. \quad (1)$$

where X_R is the mass fraction of rutile in the samples; and I_a and I_r, the integrated 101 intensities of anatase and 110 of rutile, respectively; these lines were at $2\theta \sim 26°$.

3. Results and discussion

3.1. Precursor gel characterization

Thermogravimetric and diffraction scanning calorimetry (TG–DSC) (STA 409C, Netzsch Co., Germany) were performed in air at a heating rate of 10 °C/min. The DSC curve (Fig. 1) indicated that the TiO_2 precursor gel with 1.25 mol% cerium decomposed exothermally, with sharp peaks at 228, 449 and 585 °C. The sharp and intense exothermic peak at 228 °C stems from a thermally induced anionic redox reaction of the gel wherein the citrate ion acts as reductant and nitrate or oxynitrate ions act as oxidant. The exothermic peak at 449 °C can be assigned to the further decomposition of residual carbonaceous material. The small exothermic peak at 585 °C without further weight loss can be thought to coincide with the formation of crystalline anatase phase. From the TG graph, it was observed that the metal-citric acid precursor gel exhibited weight loss up to 550 °C, and above 550 °C the weight became almost constant. Below 550 °C, the metal complex decomposed.

The IR spectrum (670 FT-IR, USA) (using KBr pellets) of the precursor gel powder with 1.25 mol% cerium showed (Fig. 2) the strong bands at around 1600 cm^{-1}, which are related to a COO^{-1} stretching mode for a bidentate complex of Ti and Ce metallic cations.[30] The bands appearing in the region 3300–2300 cm^{-1} are characteristics of citric acid stretching mode for OH groups and CH groups. The bands appearing at 1080 and 830 cm^{-1} could be attributed to the presence of nitrate ions in the precursor gel. Below

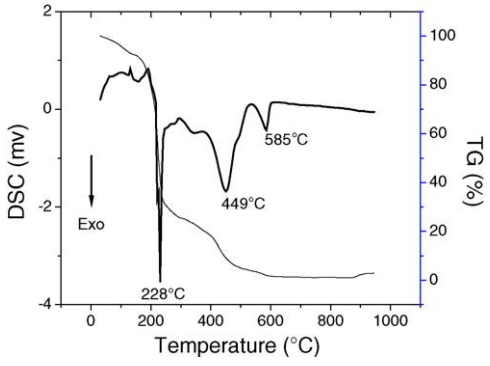

Fig. 1. TG–DSC curves of the precursor gel with 1.25 mol% cerium.

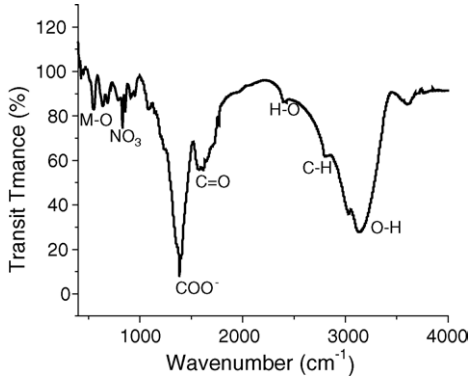

Fig. 2. IR spectra of the precursor gel with 1.25 mol% cerium.

700 cm^{-1} bands associated with metal oxygen stretching were observed.

3.2. Formation and characterization of cerium-doped anatase-type TiO_2

The X-ray diffraction (XRD; Rigaku D/Max-RB, Japan) studies of as-prepared powders with various cerium content and calcined at 550 °C for 2 h revealed (Fig. 3) that for pure TiO_2, anatase- and rutile-type structure were simultaneously present at 550 °C. The doped samples with cerium content of 1.25, 2.5 and 5 mol% were detected as single-phase anatase-type structure, and no trace of diffraction peaks due to another phase, such as cerium oxide, was detected. The CeO_2 phase was detected in the sample doped with ≥10 mol% cerium. It was supposed that the solubility of the cerium ions in the anatase-type TiO_2 at 550 °C is lower than 10 mol%.

Fig. 4 shows details of XRD patterns around $2\theta = 50°$ of the samples doped with 0, 1.25, 2.5, and 5 mol% cerium and calcined at 550 °C for 2 h. A gradual shift of the diffraction peaks of the anatase-type TiO_2 to a lower diffraction angle

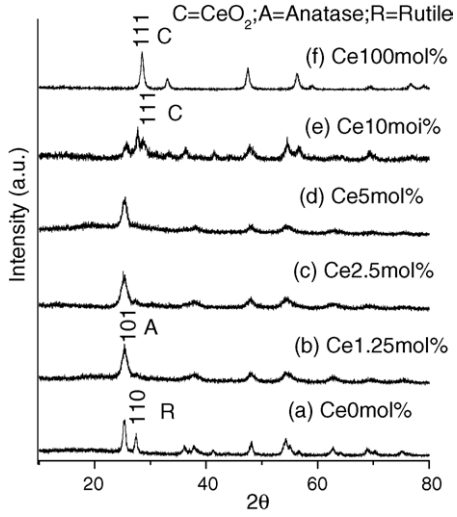

Fig. 3. XRD patterns of as-calcined powders with various amounts of cerium at 550 °C for 2 h.

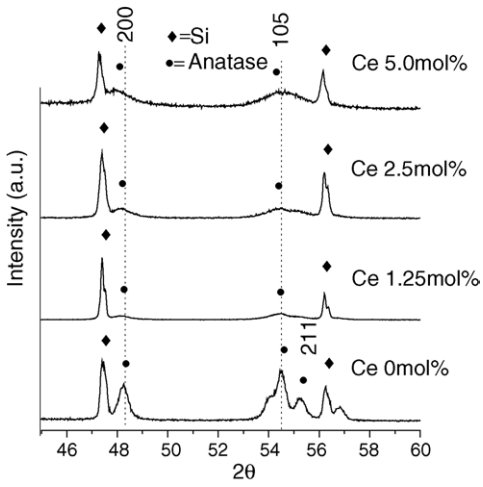

Fig. 4. Detail of the region around 50° 2θ of the XRD patterns of powders doped with various amounts of cerium.

was observed with increasing cerium content. Fig. 5 plots the lattice parameters a_0 and c_0 of the anatase-type TiO_2 as a function of cerium content. The lattice parameters a_0 and c_0 increased with increased cerium content.

The valence state of cerium ion in the powder and the powder structure were determined by X-ray photoelectron spectroscopy (XPS; VG ESCALAB MKII, UK) using the Al Kα as an excitation source with the power of 12 kV × 12 mA. The Ce 3d XPS spectra of three samples—pure CeO_2, 5 mol% and 10 mol% cerium-doped TiO_2 powder obtained from different starting compositions with 100, 5 and 10 mol% cerium(III) nitrate are shown in Fig. 6. For the three samples, the Ce 3d peaks had a binding energy of about 883 eV ($3d_{5/2}$) and about 900 eV ($3d_{3/2}$), attributed to Ce^{4+}. There was no any fitting peak of Ce^{3+} for all samples. This suggested that the Ce^{3+} was oxidized to Ce^{4+} at the calcining temperature of 550 °C or above. For pure CeO_2 and 10 mol% cerium-doped TiO_2, the Ce 3d peaks were similar and narrow (due to CeO_2 segregation in 10 mol% cerium-doped TiO_2). For 5 mol% cerium-doped TiO_2, the spectrum appeared in a wide range, due to cerium dioxide being doped in the lattice of TiO_2.[19]

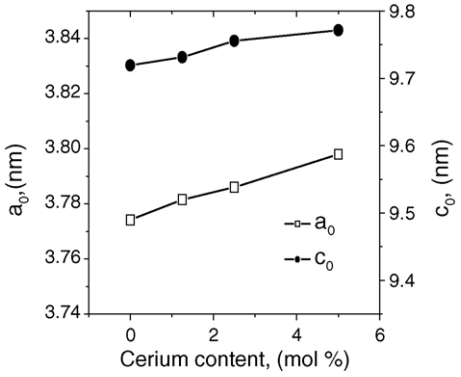

Fig. 5. Lattice parameters a_0 and c_0 of anatase-type of doped TiO_2 powders vs. cerium content.

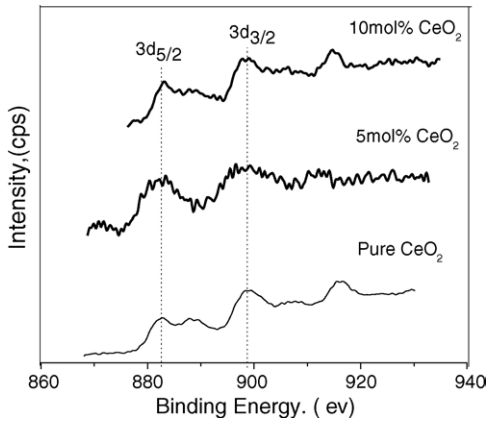

Fig. 6. XPS fitting spectra of Ce 3d on pure CeO_2, 5 and 10 mol% Ce–TiO_2.

Further information on the chemical state of cerium in the powder was obtained from transmission electron microscopy selected-area diffraction (TEM; H-800, Japan). The electron diffraction patterns of as-prepared TiO_2 doped with 1.25 and 5 mol% cerium (Fig. 7(a) and (b)) indicated that the particles of doped TiO_2 were crystalline and corresponded to the anatase phase, which suggested the absence of a small volume fraction of secondary phases.

From Fig. 3(f) and Fig. 6, it can be seen that Ce(III) can be easily oxidized to Ce(IV) under high temperature ($\geq$550 °C) condition. If cerium exists in the powder as a separate phase from anatase, it must exist as cubic CeO_2 structure by the combustion reaction of gel. It was concluded that cerium formed a solid solution with TiO_2 present in the as-prepared Ce-doped anatase-type TiO_2, which was supported by XRD data, XPS measurement results, and TEM selected-area diffraction patterns. Yue et al.[15] reported similar result.

Field emission scanning electron microscopy (FE-SEM; LEO-1450, UK) micrographs of the TiO_2 powders doped with 0, 1.25, 2.5, and 5 mol% cerium are shown in Fig. 8(a)–(d), respectively. The average particle sizes of powder estimated from FE-SEM micrographs were <30 nm, and

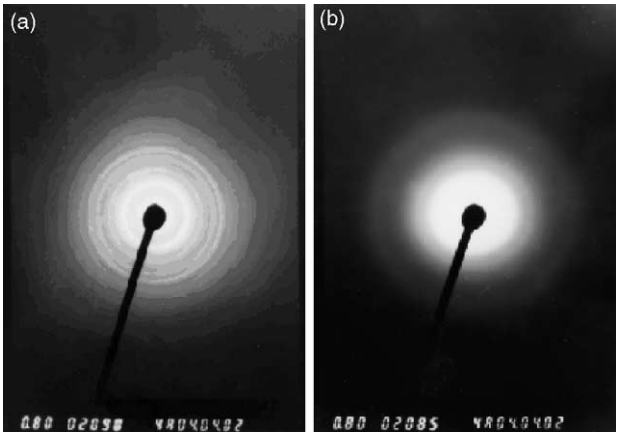

Fig. 7. TEM selected-area diffraction patterns for as-prepared Ce-doped TiO_2 powders: (a) 1.25 mol% and (b) 5 mol% cerium.

they gradually decreased in size with an increase in cerium content.

Fig. 9 plots crystallite sizes estimated from the line broadening of the (1 0 1) anatase peak in the XRD patterns as a function of cerium content in the as-prepared Ce-doped TiO_2. The crystallite size decreased from 28 to 11 nm with increased cerium content from 0 to 5 mol%. This is consistent with Ulrich's result that large amount of dopant retards coalescence of TiO_2 crystals in calcination, resulting in small crystals.[31] The particle sizes observed using FE-SEM were larger than the crystallite sizes estimated from line broadening of the XRD peak, suggesting multi-crystallite in the particle of as-prepared powder.

The UV–vis absorption spectra (UV-2401PC, Japan) were measured to correspond to the optical absorption properties of as-prepared Ce-doped TiO_2 (Fig. 10). When the cerium content was increased, onset of absorption shifted to longer wavelengths, and absorption in visible-light region over 400–500 nm and in the UV-light region was clearly observed. A more likely explanation is as follows. The quantity of photons reaching the core of a spherical particle depends on the size of the particle and the optical properties of the TiO_2 crystals. The smaller crystals are generally poorer light scatterer than larger crystals. Also, the penetration of light into the particle is influenced by the superficial morphology of the particles.[32] Particles formed from large TiO_2 crystals have smoother surface than the particles made from small crystals. On the smooth surface, the incident photons are scattered and lost mostly by reflection. The rougher surface formed by the small crystals allows a greater number of scattered photons to penetrate into the particle. From Figs. 8 and 9, it can be seen that the crystallite size and particle size of TiO_2 decreased with increased cerium content. This suggests that photon penetration into TiO_2 particles is a more likely explanation for the observed dependence of the optical absorption property on the dopant content.

3.3. Anatase–rutile phase transformation of cerium-doped TiO_2

Polymorphic transformation of ceramic materials generally depends on the nature of dopant, amount of the dopant, and the processing route. The additions of Fe_2O_3[7], $AlCl_3$[33] have been found to enhance the anatase–rutile transformation. On the other hand, Cr_2O_3[13], CeO_2[16], and SiO_2[34] have been reported to retard the anatase–rutile transformation. Phase stability of cerium-doped anatase-type TiO_2 powders by SAS was investigated.

Fig. 11 displays XRD patterns of the samples doped with various amount of cerium after they were calcined at 550–1000 °C for 2 h. These patterns showed the evolution of the anatase–rutile transformation when the calcination temperature was raised. For samples of pure and doped with 1.25 mol% cerium TiO_2 powders, only diffraction peaks due to anatase and rutile crystalline phases of TiO_2 appeared at 550–1000 °C. For sample doped with 2.5 mol% cerium and

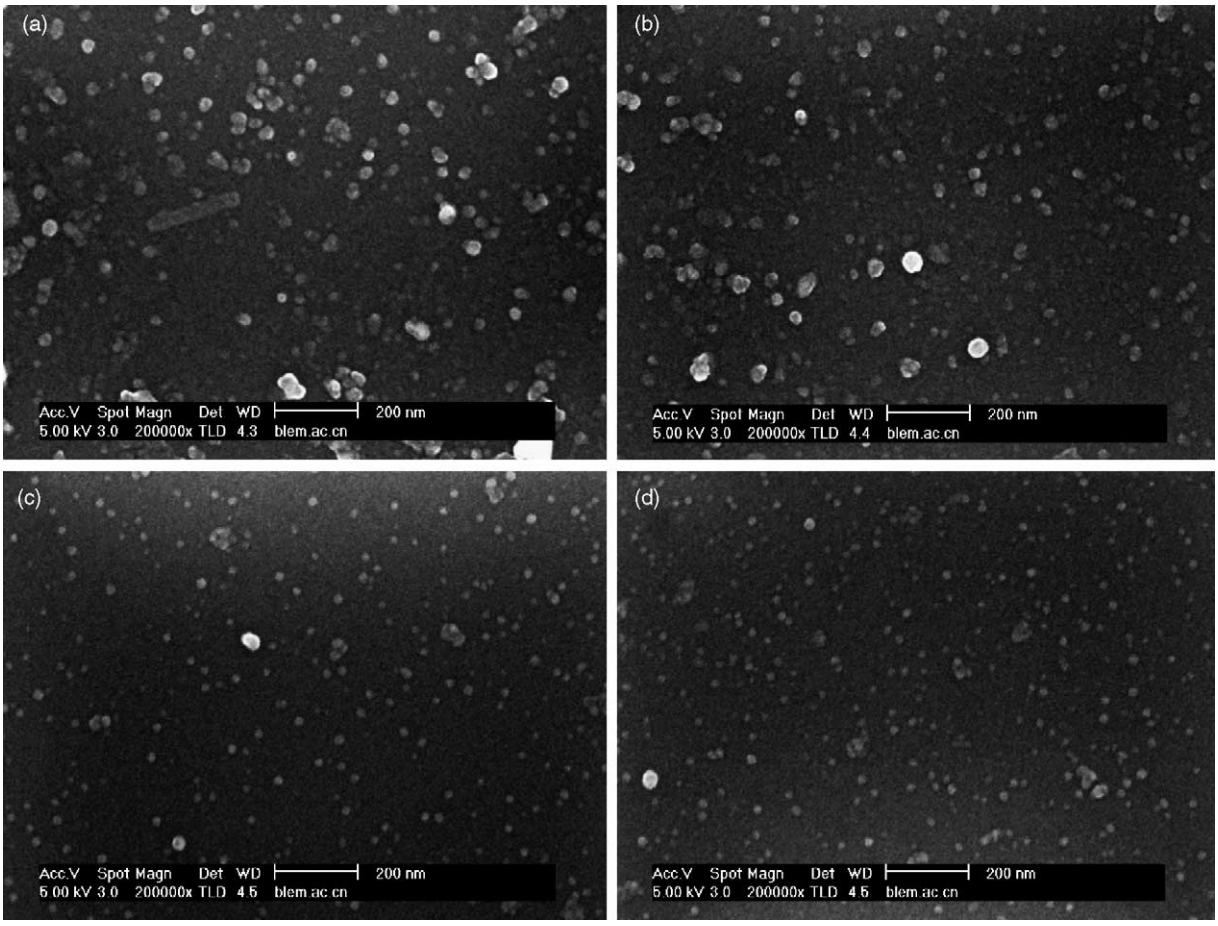

Fig. 8. FE-SEM micrographs of TiO_2 powder with various cerium contents: (a) 0 mol%; (b) 1.25 mol%; (c) 2.5 mol%; and (d) 5 mol% calcined at 550 °C for 2 h.

for sample doped with 5 mol% cerium, diffraction peaks of CeO_2 (cubic phase) were observed after the powders were calcined above 800 and 750 °C, respectively. It was supposed that residual cerium component separated from the rutile phase was crystallized as CeO_2 phase because of a much lower solubility of cerium in the rutile phase than that in the metastable anatase phase.[7] The anatase–rutile transformation ratio for the present samples as a function of heat treatment temperature is plotted in Fig. 12. The starting temperature of the phase transformation from anatase to rutile structure increased with the increase of cerium content. For sample of pure TiO_2, anatase and rutile were simultaneously present from 550 to 750 °C, while for samples doped

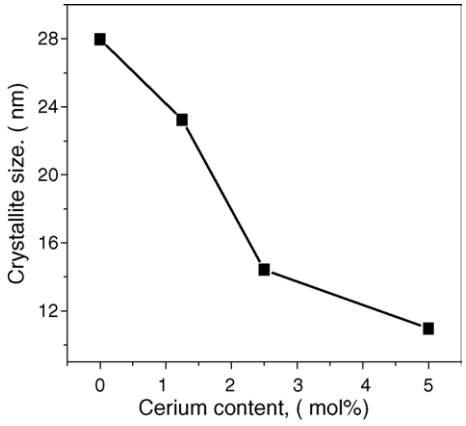

Fig. 9. Crystallite size of Ce-doped TiO_2 powder calcined at 550 °C for 2 h plotted against cerium content in the powders.

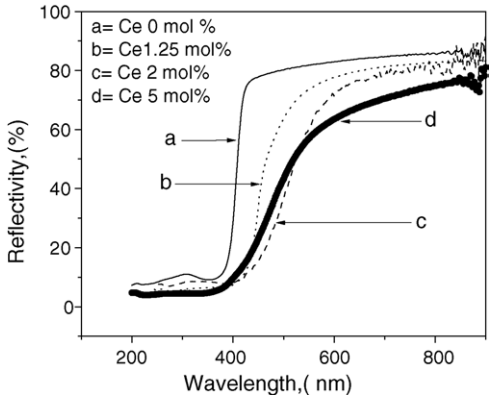

Fig. 10. Diffuse reflectance spectra of TiO_2 doped with various cerium content.

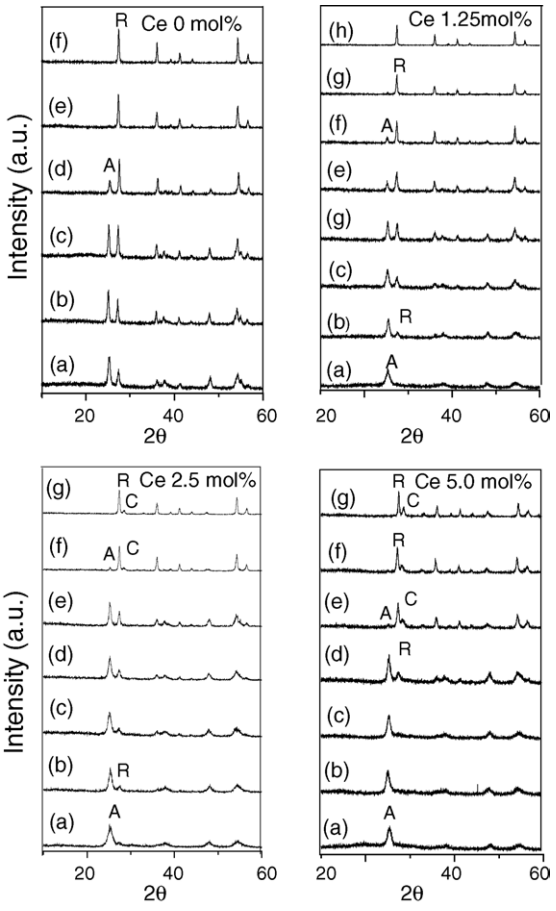

Fig. 11. XRD patterns of TiO_2 pure and doped samples obtained after calcinations for 2 h in air at: (a) 550 °C; (b) 600 °C; (c) 650 °C; (d) 700 °C; (e) 750 °C; (f) 800 °C; (g) 850 °C; and (h) 900 °C. *A*, anatase (1 0 1) reflection; *R*, rutile (1 1 0) reflection; and *C*, cerium dioxide (1 1 1) reflection.

with 1.25, 2.5 and 5 mol% cerium, the phase transformations were in the range of 600–1000, 600–850, and 700–800 °C, respectively. This proved that doping of cerium into TiO_2 retarded the anatase-type to rutile-type transformation and shifted the transformation to higher temperature. The sample with cerium content of 1.25 mol% showed a slow increase in rutile phase concentration over a wide range of temperature (∼350 °C), and the phase transformation was completed at 1000 °C. On the other hand, the 5.0 mol%-doped TiO_2 showed a narrow range of phase transformation temperature, and phase transformation started at 700 °C and completed at 800 °C. The completing temperature of transformation shifted from 1000 to 800 °C (with respect to sample with 1.25 mol% cerium) showed that cerium dioxide segregation accelerated the phase transformation of anatase to rutile due to the surface nucleation of this polymorph.[8]

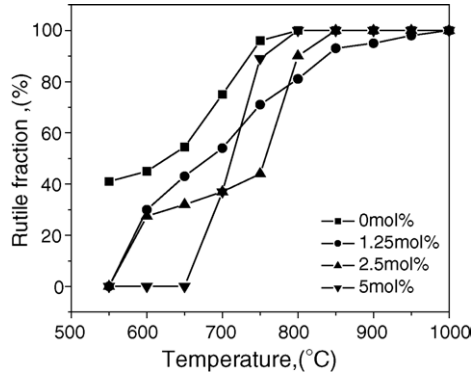

Fig. 12. Phase transformation from anatase- to rutile-type structure for TiO_2 powder with various cerium contents plotted against calcining temperature.

The influence of the dopant on the structure and textural properties of the samples can be explained based on the changes caused by the dopant on the defect structure of the TiO_2 lattice. The above XRD, XPS and TEM selected-area diffraction measurements have confirmed that cerium(IV) forms a solid solution with TiO_2. Because the ionic radius of Ce(IV) (0.092 nm) is larger than that of Ti(IV) (0.064 nm) but smaller than oxygen (0.132 nm), the cerium ions can be introduced substitutionally into the matrix, producing some deformation of the lattice structure and deformation energy;[35] this deformation energy retards the transition from anatase to rutile, producing a stabilization of the anatase phase. This can be confirmed by the above-mentioned changes of the lattice parameters of a_0 and c_0. Though cerium ions introduced substitutionally into the matrix can produce an oxygen deficiency in the crystal, which results in some extra space available to promote the anatase–rutile phase transition, the excess of oxygen deficiency produced by the dopant ions is negligible.[35] When cerium dioxide segregation occurred (samples with cerium contents of 2.5 and 5.0 mol% after calcination above 800 and 750 °C), the transformation to rutile completed at a lower temperature because the surface nucleation is favored for the dopant.

4. Conclusions

1. A new procedure was developed for the preparation of highly photoactive nano crystalline Ce-doped TiO_2 photocatalysts with anatase single-phase. One advantage of the method should be the relative ease and uniformity with which dopants and major substitutions are introduced at the solution stage. It can thus be used to prepare doped and multicomponent TiO_2-based powders.
2. The existence of Ce^{4+} in the as-prepared anatase samples and the absence of cerium dioxide as secondary phase without making a solid solution with TiO_2 in the samples were confirmed using XRD, XPS, TEM selected-area diffraction patterns.
3. Doping CeO_2 into TiO_2 not only suppressed the crystal growth of TiO_2 but also prevented phase transition of anatase to rutile. When cerium dioxide segregation occurred, the rutile formation was accelerated during phase transformation from anatase to rutile.
4. The Ce^{4+}-doped TiO_2 samples showed strong absorption in the UV–vis range and a red shift in the band gap transition.

References

1. Stiller, S., Gers-Barlag, H., Lergenmueller, M., Pflücker, F., Schulz, J., Wittern, K. P. *et al.*, Investigation of the stability in emulsions stabilized with different surface modified titanium dioxides. *Colloid Surf. A*, 2004, **232**, 261–267.
2. Richards, B. S., Rowlands, S. F., Ueranatasun, A., Cotter, J. E. and Honsberg, C. B., Potential cost reduction of buried-contact solar cells through the use of titanium dioxide thin films. *Sol. Energy*, 2004, **76**, 269–276.
3. Ruiz, A. M., Sakai, G., Cornet, A., Shimanoe, K., Morante, J. R. and Yamazoe, N., Cr-doped TiO_2 gas sensor for exhaust NO_2 monitoring. *Sens. Actuators B: Chem.*, 2003, **93**, 509–518.
4. Ana, I., Cardona, Roberto, C., Benigno, S., Pedro, Á. and Moisés, R., TiO_2 on magnesium silicate monolith: effects of different preparation techniques on the photocatalytic oxidation of chlorinated hydrocarbons. *Energy*, 2004, **29**, 845–852.
5. Larsson, P. O. and Andersson, A., Complete oxidation of CO, ethanol, and ethyl acetate over copper oxide supported on titania and ceria modified titania. *J. Catal.*, 1998, **179**, 72–89.
6. Kamat, P. V. and Dimitrijevic, N. M., Colloidal semiconductors as photocatalysts for solar energy conversion. *Sol. Energy*, 1990, **44**(2), 83–98.
7. Hirano, M., Joji, T. and Inagaki, M., Direct formation of iron(III)-doped titanium oxide (anatase) by thermal hydrolysis and its structural property. *J. Am. Ceram. Soc.*, 2004, **87**(1), 35–41.
8. Inagaki, M., Nakazawa, Y., Hirano, M., Kobayashi, Y. and Toyoda, M., Preparation of stable anatase-type TiO_2 and its photocatalytic performance. *Int. J. Inorg. Mater.*, 2001, **3**(7), 809–811.
9. Arroy, R., Cordoba, G., Padilla, J. and Lara, V. H., Influence of manganese ions on the anatase–rutile phase transition of TiO_2 prepared by the sol–gel process. *Mater. Lett.*, 2002, **54**, 397–402.
10. Ivanova, T., Harizanova, A., Surtchev, M. and Nenova, Z., Investigation of sol–gel derived thin films of titanium dioxide doped with vanadium oxide. *Sol. Energy Mater. Sol. C*, 2003, **76**, 591–598.
11. Shivalingappa, L., Sheng, J. and Fukami, T., Photocatalytic effect in platinum doped titanium dioxide films. *Vacuum*, 1997, **48**(5), 413–416.
12. Ranjit, K. T., Willner, I., Bossmann, S. H. and Braun, A. M., Lanthanide oxide doped titanium dioxide photocatalysts effective photocatalysts for the enhanced degradation of salicylic acid and t-cinnamic acid. *J. Catal.*, 2001, **204**, 305–313.
13. Wilke, K. and Breuer, H. D., The influence of transition metal doping on the physical and photocatalytic properties of titanium. *J. Photochem. Photobiol. A: Chem.*, 1999, **121**, 49–53.
14. Yu, X. Y., Cheng, J. J., Yang, Y. and Du, Y. J., Effects of rare earth oxide doping on the photocatalytic activities of TiO_2. *J. East Chin. Univ. Sci. Technol.*, 2000, **26**(3), 287–289.
15. Yue, L. H., Shui, M., Xu, Z. D. and Zheng, Y. F., The a-r transformation and photocatalytic activities of mixed TiO_2 rare earth oxides. *J. Zhejiang Univ.*, 2000, **27**(1), 69–74 (Science Edition).
16. Jing, L. Q., Sun, X. J., Cai, W. M., Li, X. Q., Fu, H. G., Hou, H. G. *et al.*, Photoluminescence of Ce doped TiO_2 nanoparticles and their photocatalytic activity. *Acta Chim. Sin.*, 2003, **8**, 1241–1245.
17. Wang, Y. M., Liu, S. W., Lü, M. K., Wang, S. F., Gu, F., Gai, X. Z. *et al.*, Preparation and photocatalytic properties of Zr^{4+}-doped TiO_2 nano-crystals. *J. Mol. Catal. A: Chem.*, 2004, **215**, 137–142.
18. Zhang, Y. H. and Reller, A., Investigation of mesoporous and microporous nanocrystalline silicon-doped titania. *Mater. Lett.*, 2003, **57**, 4108–4113.
19. Li, X. Z., Li, F. B., Yang, C. L. and Ge, W. K., Photocatalytic activity of WO_x–TiO_2 under visible light irradiation. *J. Photochem. Photobiol. A: Chem.*, 2001, **141**, 209–217.
20. Turković, A., Grazing-incidence small-angle X-ray scattering and reflectivity on nanostructured oxide films. *Mater. Sci. Eng. B*, 2004, **110**, 68–78.
21. Duran, P., Capel, F., Gutierrez, D., Tartaj, J. and Moure, C., Cerium(IV) oxide synthesis and sinterable powders prepared by polymeric organic complex solution method. *J. Eur. Ceram. Soc.*, 2002, **22**, 1711–1721.
22. Luo, S., Tang, Z., Yao, W. H. and Zhang, Z. T., Low-temperature combustion synthesis and characterization of nanosized tetragonal barium titanate powders. *Microelectron. Eng.*, 2003, **66**, 147–152.
23. Marinsek, M., Zupan, K. and Maeek, J., Ni-YSZ cermet anodes prepared by citrate/nitrate combustion synthesis. *J. Powder Sources*, 2002, **106**, 178–189.
24. Chakraborty, A., Devi, P. S., Roy, S. and Maiti, H. S., Low-temperature synthesis of ultrafine $La_{0.84}Sr_{0.16}MnO_3$ powder by an autoignition process. *J. Mater. Res.*, 1994, **9**(4), 986–991.
25. Schäfer, J., Sigmund, W., Roy, S. and Aldinger, F., Low temperature synthesis of ultrafine Pb(Zr, Ti)O_3 powder by sol–gel combustion. *J. Mater. Res.*, 1997, **12**(10), 2518–2521.
26. Ringuedé, A., Labrincha, J. A. and Frade, J. R., A combustion synthesis method to obtain alternative cermet materials for SOFC anodes. *Solid State Ionics*, 2001, **141**(142), 549–557.
27. Bamwenda, G. R., Uesigi, T., Abe, Y., Sayama, K. and Arakawa, H., The photocatalytic oxidation of water to O_2 over pure CeO_2, WO_3, and TiO_2 using Fe^{3+} and Ce^{4+} as electron acceptors. *Appl. Catal. A: Gen.*, 2001, **205**, 117–128.
28. Gablenz, S., Abicht, H. P., Pippel, E., Lichtenberger, O. and Woltersdorf, J., New evidence for an oxycarbonate phase as an intermediate step in $BaTiO_3$ preparation. *J. Eur. Ceram. Soc.*, 2000, **20**, 1053–1060.
29. Spurr, R. A. and Myers, H., Quantitative analysis of anatase–rutile mixtures with an X-ray diffractometer. *Anal. Chem.*, 1957, **29**, 760–763.
30. Nakmoto, K., trans. D.R. Huang, R.C. Wang, *Infrared and Raman Spectra of Inorganic and Coordination Compounds (third ed.)*. Chemical Industry Press, Beijing, 1986, p. 242.
31. Gesenhues, U., Doping of TiO_2 pigments by Al^{3+}. *Solid State Ionics*, 1997, **101–103**, 1171–1180.
32. Maira, A. J., Yeung, K. L., Lee, C. Y., Yue, P. L. and Chan, C. K., Size effect in gas-phase photo-oxidation of trichloroethylene using nanometer-sized TiO_2 catalysts. *J. Catal.*, 2000, **192**, 185–196.
33. Gesenhues, U. and Rentshler, T., Crystal growth and defect structure of Al^{3+}-doped rutile. *J. Solid State Chem.*, 1999, **143**, 210–218.
34. Zhou, Y. S. and Fan, X. H., Preparation and properties of the nanometer composite oxide TiO_2–SiO_2. *Chem. J. Chin. U*, 2003, **7**, 1266–1270.
35. Rodriguez, R., Vargas, S., Arroyo, R., Montiel, R. and Haro, E., Modification of the phase transition temperatures in titania doped with various cations. *J. Mater. Res.*, 1997, **12**(2), 439–443.